

## Bubble Motion in the Nonlinear Rayleigh-Taylor Instability

H. J. Kull

*Technische Hochschule Darmstadt, Institut für Angewandte Physik, D-6100 Darmstadt,  
Federal Republic of Germany*

(Received 6 May 1983)

An approximate description of Rayleigh-Taylor bubble motion is given in terms of a Fourier series expansion of the velocity potential. Consistent predictions for the steady-state velocity, the bubble curvature, and the first three Fourier coefficients are obtained. A simple model of nonsteady bubble motion is developed. It is found that an exponential amplitude dependence is responsible for a rapid transition to the steady-state regime when the amplitude becomes larger than  $\sim \lambda/6\pi$ .

PACS numbers: 47.20.+m, 52.35.Mw

Rayleigh-Taylor-type hydrodynamic instabilities are under current investigation in inertial confinement fusion physics.<sup>1-3</sup> The growth of these instabilities may limit the fusion gain for thin shell pellets by destroying the spherical implosion symmetry. In a number of hydrodynamic simulation studies<sup>4-6</sup> it has been observed that nonlinearities play a major role in reducing the classical instability growth rates. After an initial phase of exponential growth the instability evolves in the nonlinear regime into an approximate steady state of rising bubbles. This final steady state is well known from early experiments<sup>7-9</sup> and the steady-state velocity was given with high accuracy by the theories of Birkhoff and Carter<sup>10</sup> and Garabedian.<sup>11</sup>

It is the purpose in this paper to give an approximate description of Rayleigh-Taylor (RT) bubble motion in plane potential flow. The method used here is based on a Fourier series expansion of the velocity potential in a coordinate frame comoving with the bubbles. In this frame the Fourier coefficients saturate at their steady-state values. It will be assumed that these are rapidly decreasing with the mode number so that accurate approximations can be obtained by determining the first few harmonics only. The technique is applied to the steady-state regime and consistent predictions for the first three Fourier coefficients, the bubble velocity, and the bubble curvature are derived. One can also easily extend the model to account for the nonsteady phase of bubble formation. Here nonlinearities are found to become important in the very early stages of the instability which can explain the striking departures from linear theory observed in numerical calculations.<sup>4-6</sup> After this work was completed I noticed that a similar concept has been used before by Layzer.<sup>12</sup> In the present treatment a more rigorous justification of the procedure is

given by the third-order steady-state theory and the nonsteady growth is derived for slightly more general initial conditions.

Consider a half-infinite fluid layer supported by gas pressure under gravity and assume plane potential flow periodic in the  $x$  direction with wave number  $k$  and uniform gravitational acceleration  $g$  along the  $(-z)$  direction. For convenience dimensionless variables are used with all lengths and times measured in units of  $k^{-1}$  and  $(gk)^{-1/2}$ , respectively, and an accelerated coordinate frame is chosen with the origin attached to the bubble vertex. Then the basic equations governing the flow assume the form

$$\varphi(x, z, t) = \sum_{m=1}^{\infty} \varphi_m(t) [\cos(mx) e^{-mz} - 1 + mz], \quad (1a)$$

$$w + \frac{1}{2}(u^2 + v^2) + (1 + \ddot{a})\xi = 0, \quad (1b)$$

$$\partial_t \xi + u \partial_x \xi - v = 0, \quad (1c)$$

with

$$u = \partial_x \varphi|_{z=\xi}, \quad v = \partial_z \varphi|_{z=\xi}, \quad w = \partial_t \varphi|_{z=\xi},$$

where the dot denotes the time derivative and  $a(t)$  the bubble amplitude relative to the undisturbed surface. In Eq. (1a) the velocity potential  $\varphi(x, z, t)$  is expressed as a Fourier series in  $x$  which satisfies the Laplace equation and the boundary conditions  $\varphi = \partial_z \varphi = 0$  at the origin  $x = z = 0$ . The expansion coefficients  $\varphi_m(t)$  are subject to the nonlinear free-surface boundary condition (1b). It follows immediately from Bernoulli's equation if the surface pressure is taken constant and if the bubble acceleration  $\ddot{a}(t)$  is added to the usual gravitational acceleration. The equation of the free surface  $z = \xi(x, t)$  is determined from the requirement that surface particles move with the fluid as expressed by Eq. (1c). In terms of the Fourier expansion (1a) the bubble velocity is giv-

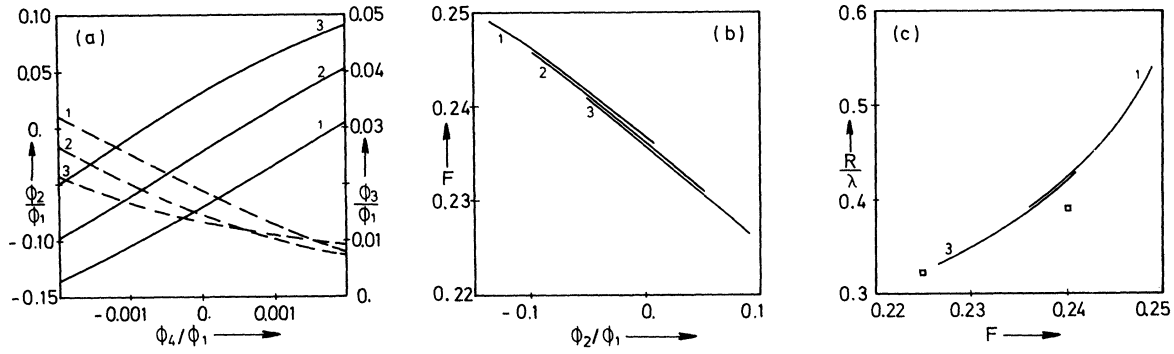


FIG. 1. (a) First ( $\varphi_2$ ) and second ( $\varphi_3$ , dashed lines) harmonic as determined by Eqs. (5b) and (5c). In the present model the amplitudes of higher harmonics are varied within a given range to account for their occurrence in the spike solution:  $|\varphi_4/\varphi_1| < 2 \times 10^{-3}$ ,  $\varphi_5/\varphi_1 = -0.0002$  (curve 1), 0 (curve 2),  $+0.0002$  (curve 3). (b) Froude number as a function of  $\varphi_2$ . Note that for given  $\varphi_2$  one finds only minor variations with  $\varphi_5$  (curves 1–3). (c) Radius of curvature  $R$  vs Froude number  $F$ . Comparison is made with the data of Refs. 4 and 6 at  $F = 0.24$  and  $F = 0.225$ , respectively.

en by

$$\dot{a}(t) = -\partial_z \varphi|_{z \rightarrow +\infty} = -\sum_{m=1}^{\infty} m \varphi_m(t). \quad (2)$$

To satisfy Eq. (1) in a neighborhood of the vertex  $x=0$ , we expand the potential (1a), the surface displacement  $\zeta(x, t)$ , and the velocity components  $u, v$  in power series of the form

$$\begin{aligned} \varphi(x, z, t) &= \sum_{i=0}^{\infty} \sum_{j=0}^{\infty} \frac{(-1)^{i+j}}{(2i)!j!} b_{2i+j}(t) x^{2i} z^j - b_0(t) + b_1(t)z, \\ \zeta(x, t) &= \sum_{i=1}^{\infty} \frac{(-1)^i}{(2i)!} c_i(t) x^{2i}, \quad u(x, t) = -b_2 x + \alpha x^3 + \beta x^5 + O(x^7), \quad v(x, t) = \gamma x^2 + \delta x^4 + \eta x^6 + O(x^8), \end{aligned} \quad (3)$$

with the expansion coefficients given by

$$\begin{aligned} b_i(t) &= \sum_{m=1}^{\infty} m^i \varphi_m, \quad \alpha = \frac{1}{3!}(b_4 - 3b_3 c_1), \quad \gamma = \frac{1}{2}(b_3 - b_2 c_1), \quad \beta = \frac{-1}{5!}(b_6 - 10b_5 c_1 + 15b_4 c_1^2 - 5b_3 c_2), \\ \delta &= \frac{-1}{4!}(b_5 - 6b_4 c_1 + 3b_3 c_1^2 - b_2 c_2), \quad \eta = \frac{1}{6!}(b_7 - 15b_6 c_1 + 45b_5 c_1^2 - 15b_4 c_2 - 15b_4 c_1^3 + 15b_3 c_1 c_2 - b_2 c_3). \end{aligned}$$

We first restrict attention to steady-state conditions where one has  $\partial_t \zeta = w = \dot{a} = 0$ . Inserting here the series (3) into Eqs. (1b), (1c), and equating the coefficients of equal powers of  $x$  one finds up to the order  $O(x^6)$  the relations

$$b_2 c_1 - \gamma = 0, \quad b_2^2 - c_1 = 0, \quad O(x^2) \quad (4a)$$

$$c_2 b_2 + 3! \alpha c_1 + 3! \delta = 0, \quad 4! \alpha b_2 - \frac{4!}{2} \gamma^2 - c_2 = 0, \quad O(x^4) \quad (4b)$$

$$c_3 b_2 + 20 \alpha c_2 - 5! \beta c_1 - 5! \eta = 0, \quad \frac{6!}{2} \alpha^2 - 6! \beta b_2 + 6! \gamma \delta - c_3 = 0, \quad O(x^6). \quad (4c)$$

Eliminating now the coefficients  $c_1, c_2, c_3$  from Eq. (4) yields after some algebra the system

$$b_3 - 3b_2^3 = 0, \quad (5a)$$

$$95b_3^3 - 90b_2 b_3 b_4 + 9b_2^2 b_5 = 0, \quad (5b)$$

$$105b_3^5 - 840b_4 b_3^3 b_2 + 882b_5 b_3^2 b_2^2 - 63b_5 b_4 b_2^3 - 189b_6 b_3 b_2^3 + 9b_7 b_2^4 = 0. \quad (5c)$$

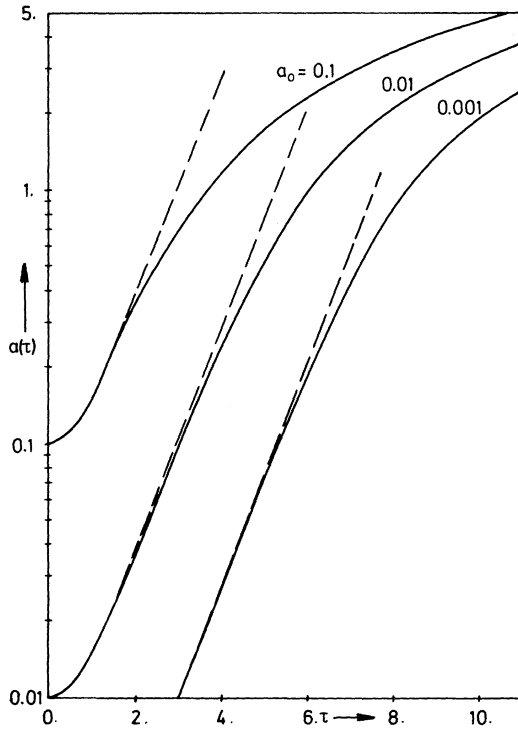


FIG. 2. Time evolution of the bubble amplitude for the initial conditions  $a_0 = 0.1, 0.01, 0.001, \dot{a}_0 = 0$ . The dashed lines correspond to classical growth  $a(t) = a_0 \cosh t$ .

Now proceed by solving Eqs. (5a)–(5c) for the first three Fourier coefficients with the others assuming given values. Introducing the ratios  $\varphi_i' = \varphi_i / \varphi_1, b_i' = b_i / \varphi_1$ , Eq. (5a) is easily solved for  $\varphi_1$  yielding

$$\varphi_1^2 = b_3' / 3b_2'^3, \tag{6}$$

and Eqs. (5b) and (5c) depend on primed quantities only. The latter have been solved numerically for  $\varphi_2'$  and  $\varphi_3'$  in the parameter range  $|\varphi_3'| < 0.1, |\varphi_4'| < 2 \times 10^{-3}, |\varphi_5'| < 2 \times 10^{-4}, \varphi_i' = 0$  for  $i > 5$ . The result proves consistent with the assumption of rapidly decreasing harmonics [Fig. 1(a)]. The first harmonic is found to be smaller than  $\sim 0.15|\varphi_1|$  and the second smaller than  $\sim 0.03 \times |\varphi_1|$ . It is also noted that  $\varphi_2$  can assume both positive and negative values while  $\varphi_3$  always stays positive. It may therefore be possible to find solutions where  $\varphi_3$  is the first nonvanishing harmonic contribution. For any solution for  $\varphi_2', \varphi_3'$ , Eqs. (2) and (6) determine the corresponding bubble velocity. It is usual to express  $\dot{a}$  by the related Froude number  $F = \dot{a} / (2\pi)^{1/2}$  which is shown in Fig. 1(b) as a function of  $\varphi_2'$ . In the present calculation the Froude number shows variations

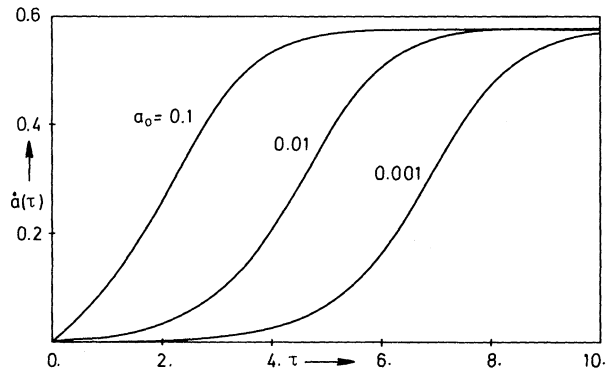


FIG. 3. Bubble velocity for the same parameters as Fig. 2. In the nonlinear regime the curves approach the asymptotic value  $1/\sqrt{3}$ .

from  $\sim 0.225$  to  $\sim 0.25$  in close agreement with previous results.<sup>10,11</sup> One should also notice that large Froude numbers occur for negative values of  $\varphi_2'$  when the phases of the first harmonic and the fundamental mode are opposed. At much larger harmonic amplitudes a similar dependence has been observed recently.<sup>3</sup> It is also of interest to discuss the radius of curvature at the bubble vertex,

$$\frac{R}{\lambda} = \frac{1}{2\pi c_1} = \frac{3}{2\pi} \frac{b_2'}{b_3'}, \tag{7}$$

in the present model. It can be shown that it increases with the possible Froude numbers and varies between  $\sim 0.3$  and  $\sim 0.5$  [Fig. 1(c)]. For comparison data given in Refs. 4 and 6 have been indicated in Fig. 1(c).

Based on the analysis of the steady state one can also consider a simple model of nonsteady bubble motion. As a first estimate we neglect all harmonic contributions and use Eqs. (1b) and

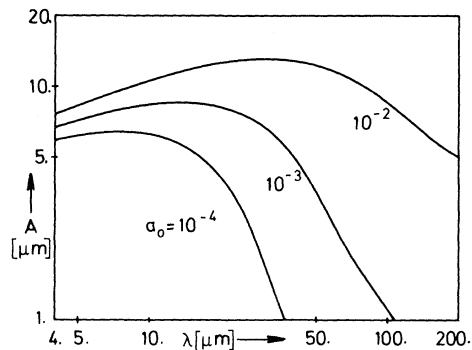


FIG. 4. Final amplitude as a function of the wavelength. In the nonlinear case a wavelength of maximum growth is obtained.

(1c) up to the order  $x^2$  for determining the fundamental mode  $\varphi_1$ . Truncating the series under Eqs. (2) and (3) after  $m = 1$  one has  $b_i = -\dot{a}$  and Eqs. (1b) and (1c) can be written consistent up to the order  $x^2$  as

$$\ddot{a} + \frac{\dot{a}^2}{1 - c_1} - \frac{c_1}{1 - c_1} = 0, \quad \dot{c}_1 - \dot{a}(1 - 3c_1) = 0. \quad (8)$$

Equation (8) represents a nonlinear equation of motion for the bubble amplitude  $a(t)$ . It has a first integral of the form

$$\dot{a}^2 = \frac{\frac{2}{3}\{1 - \exp[-3(a - a_0)]\} - e^{-3a}\{2(a - a_0) - \dot{a}_0^2[1 + 2\exp(3a_0)]\}}{2 + e^{-3a}}, \quad (9)$$

with the initial conditions  $\dot{a}(0) = \dot{a}_0 \ll 1$ ,  $a(0) = c_1(0) = a_0 \ll 1$ . The bubble velocity as given by Eq. (8) shows a strong exponential amplitude dependence. For small amplitudes ( $3a \ll 1$ ) it reduces to the well-known result of linear theory,

$$\dot{a}^2 = a^2 - (a_0^2 - \dot{a}_0^2), \quad a = a_0 \cosh t + \dot{a}_0 \sinh t. \quad (10)$$

In the opposite limit of large amplitudes one obtains a constant steady-state velocity with the Froude number  $1/(6\pi)^{1/2} \cong 0.230$ . The transition from the linear to the steady-state regime occurs for  $3a \sim 1$  when the bubble amplitude becomes  $\sim \lambda/(6\pi)$ . This value is considerably lower than previous estimates (0.4).<sup>7</sup> For an evaluation of Eq. (9) we refer to Figs. 2 and 3 where  $a(t)$  and  $\dot{a}(t)$  are shown for the initial conditions  $a_0 = 0.1, 0.01, 0.001, \dot{a}_0 = 0$ .

We finally discuss the wavelength dependence of the final bubble amplitude  $A$  as given by

$$A(\lambda) = (\lambda/2\pi)a(p/\sqrt{\lambda}), \quad (11)$$

where  $p = (4\pi g t^2/2)^{1/2}$  now is considered as a fixed parameter and where all quantities here have their usual dimensions. In Fig. 4,  $A(\lambda)$  is shown for  $p = 50$  ( $\mu\text{m}$ )<sup>1/2</sup>. Since shorter wavelengths are favored by the linear regime but larger ones by the final steady state maximum growth occurs for intermediate wavelengths which are here of the order of 10–50  $\mu\text{m}$ . In the present example an accelerated foil could be pushed the distance

$gt^2/2 \cong 200$   $\mu\text{m}$  which is about twenty times the maximum bubble amplitude.

I wish to thank P. Mulser for many helpful discussions. This work was supported by the Bundesministerium für Forschung und Technologie.

<sup>1</sup>R. L. McCrory, L. Montierth, R. L. Morse, and C. P. Verdon, *Phys. Rev. Lett.* **46**, 336 (1981).

<sup>2</sup>M. H. Emery, J. H. Gardner, and J. P. Boris, *Phys. Rev. Lett.* **48**, 677 (1982).

<sup>3</sup>C. P. Verdon, R. L. McCrory, R. L. Morse, G. R. Baker, D. I. Meiron, and S. A. Orszag, *Phys. Fluids* **25**, 1653 (1982).

<sup>4</sup>F. H. Harlow and J. E. Welch, *Phys. Fluids* **9**, 842 (1966).

<sup>5</sup>B. J. Daly, *Phys. Fluids* **10**, 297 (1967), and **12**, 1340 (1969).

<sup>6</sup>G. R. Baker, D. I. Meiron, and S. A. Orszag, *Phys. Fluids* **23**, 1485 (1980).

<sup>7</sup>D. J. Lewis, *Proc. Roy. Soc. London, Ser. A* **202**, 81 (1950).

<sup>8</sup>R. M. Davies and G. Taylor, *Proc. Roy. Soc. London, Ser. A* **200**, 375 (1950).

<sup>9</sup>H. W. Emmons, C. T. Chang, and B. C. Watson, *J. Fluid Mech.* **7**, 177 (1960).

<sup>10</sup>G. Birkhoff and D. Carter, *J. Math. Mech.* **6**, 769 (1957).

<sup>11</sup>P. R. Garabedian, *Proc. Roy. Soc. London, Ser. A* **241**, 423 (1957).

<sup>12</sup>D. Layzer, *Astrophys. J.* **122**, 1 (1955).